American Journal of Engineering Research (AJER)
E-ISSN: 2320-0847 p-ISSN: 2320-0936
Volume-8, Issue-3, pp-107-114
www.ajer.org
Research Paper Open Access

Use of Flexibility Absolute Difference Index to Detect Bracing Effects in a Steel Frame Model

Ai D. Nguyen[1], Elizabeth K. Ervin[2]
[1](M.S., Civil Engineering, University of Mississippi, USA)
[2](Associate Professor, Civil Engineering, University of Mississippi, USA)
Corresponding Author: Elizabeth K. Ervin

ABSTRACT :*When civil infrastructure is inspected, the cost can be high and service is often impaired. Improved inspection techniques are required to reduce the cost, time, and subjectivity. A quantitative metric based upon objective data would be useful in augmenting visual inspection with a non-invasive dynamic analysis. A software package developed in-house employs vibration data to improve damage detection techniques. The final result is color coded visualization of location hotspots with relative change valuations. The ultimate goal is to measure global stability effects to eventually assist in predicting and preventing critical failure.*

This work uses ABAQUS finite element output for change detection in a laboratory-sized steel frame model. The damage sensitive feature of flexibility combined with an absolute difference algorithm is examined herein on structural shoring changes. The index is used to measure global reinforcement effects of sway bracing in diagonal, two-faced, and cross configurations. These bracing studies generate five configurations and eleven comparisons, completing a sensitivity analysis on Flexibility Absolute Difference. This index worked well for these braced structures and performed slightly better when low frequency modes were dominant. Fundamental modes of lower frequencies are most important for global motion, so this result is consistent with dynamic theory.

KEYWORDS *structural health monitoring, infrastructure inspection, big data extraction, damage assessment*

Date of Submission: 20-02-2019 Date of acceptance: 08-03-2019

I. INTRODUCTION

The nation requires objective and reliable inspection techniques especially since the American infrastructure is essential to both national economy and defense. The Federal Highway Administration (FHWA) requires evaluation of all bridges; however, it does not consider regarding cost, return period, or health evaluation. The FHWA estimates federal biennial inspection fees are 2.7 billion dollars. The Mississippi Department of Transportation (MDOT) Bridge Safety Inspection Policy and Procedure Manual schedules routine inspection for each state bridge every 24 months [1]. The average unit cost of Mississippi highway bridge inspections is $57 per square foot, which is less than the national estimate [2]. Additionally, local county or city bridge inspection standards vary widely. With so many bridges needing inspection every year, evaluations should be both low cost and high quality.

Currently, bridges and buildings must be physically and visually inspected. While a structure is under inspection, its usage is affected. Bridge traffic may have to detour or a building may have to close. Moreover, visual inspection has limitations to local surface defects in viewable areas. Methods such as the ultrasonic, liquid penetrant, and radiography, non-destructive testing tends to investigate internal structures but only local area often due to great cost. Since time is money, faster techniques with broader reach would better serve current American infrastructure needs.

The basis of this work is vibration as viewed in the frequency domain. Temporal measurements can vary widely, so frequency information is often employed. Natural frequencies and mode shapes are the Eigenvalues and Eigenvectors of a multiple degree of freedom (i.e. number of measurement nodes) system. Since every structure has its individual natural frequencies, shifts in resonant frequency and deflective shapes can be used to determine if, how much, and where damage occurs. Literature proposes several damage detection techniques, but not all have three-dimensional physical meanings. Stiffness and its inverse flexibility have physical meanings and thus make for the prime initial study.

Damage detection is comparing two states of a structure: a baseline "prior" case and a damaged "current" case. Technically, damage indices quantify change, so damage and reinforcement detection follow the same procedure. This work will apply the Flexibility Absolute Difference (FAD) index to evaluate both symmetric and asymmetric configurations of structural sway bracing: diagonal, two-faced, and cross bracing.

II. PRIOR EXPERIMENT

Shown in Figure 1a, a structure was built in the Multi-Function Dynamics Laboratory (MFDL) at the University of Mississippi. The main frame was entirely made from standard size C-shaped galvanized steel UNISTRUT®. The two-story structure was nominally 4-foot by 4-foot in plane, 5.5 feet in height and supported by four 5-gallon buckets cast in place with 28-day cured concrete foundations. The columns and beams were oriented to face the center of the building, and the four sides named by location of North (N), East (E), South (S), and West (W). The origin coordinate of the system was set at the bottom of the Southwest column [3].

Modal tap testing was performed on this frame. As shown in Figure 1b, sensors captured accelerations at 52 measurement nodes. Each beam consisted of five nodes, except the bottom floor beams, which had only three nodes. The columns had six nodes each to capture global motions. The nodes were numbered from the origin in a counter-clockwise fashion from bottom to top. These locations are consistent and significant to the work herein, but note that no experimental data is employed.

III. PROCEDURE

ABAQUS/CAE® or familiarly "ABAQUS" is a diverse finite element analysis software package for computer-aided engineers [4]. The three steps of generating any model are pre-processing, simulating, and post-processing; model construction was the best attempt to noiselessly represent the experimental structure, and output tables were post-processed in several manners. The cross-section properties were those of the UNISTRUT with proper rotations. Members were assembled into a frame. Boundary conditions were set to X and Y displacements of 0.1 inch and rotations of 0.02 radian, respectively, while thresholds on Z displacement was 0.01 inch and rotation was 0.002 radian. These selected values best fit the natural frequencies of the experimental structure.

The analysis mesh was globally seeded at one inch spacing, which was more refined than the sensor mesh. Analysis output was later transformed to coordinating measurement nodal output. With the Step Module set to Linear Perturbation/Frequency, thirty eigenvalues (natural frequencies) were found along with their corresponding thirty eigenvectors (mode shapes). The translational and rotational displacements of the eigenvectors are output as a text Field Table with the extension .RPT. These results are reformatted into a comma separated value .CSV format for input to Structural Health Evaluation^TM, named SHE^TM for short. Written in MATLAB® [5], this in-house software loads any frequency domain information without considering material modeling or crossection geometries.

Each mode shape's 52 nodal deflections contain general three-dimensional spatial relationships. Similarity of mode shapes can then be matched through human observation, especially when decoupled by ABAQUS. The most difficult and only subjective part of the process, mode matching involves careful examination to match mechanisms, such as sway, bending, or torsion. Admittedly, this process requires structural insight, and future efforts are working to automate this for industrial applications.

Once the modes are matched, some structural damage sensitive feature must be selected. The Structural Identification field aims to fully determine each structural parameter set. In contrast, the damage detection field uses the combinatorial output while the stiffness of a system is unknown. Flexibility however can be measured, as in Sung for a multiple story building to detect modal flexibility changes [6]. Koo used modal flexibility to detect the damage of a steel bridge structure under the temperature variations. In this research, he identified the modal flexibility matrix by acceleration measurements and bending deflections for multiple damage and temperature cases [7].

Modal flexibility is defined as

$$F_{ij} = \frac{1}{\omega_i^2} \Phi_{ij} \Phi_{ij}^T \qquad \text{(Equation 1)}$$

where ωi is the natural frequency and j is the node number. True flexibility requires knowledge of a mass matrix, but herein output only methods are presented. Thus, the modal flexibility is a proportional measure of modal contribution normalized by frequency.

In this research, flexibility is used to measure change between two states with Sabatino's metric Flexibility Absolute Difference (FAD) [8]:

$$\Delta F_{ij} = \left|F_{ij} - F_{ij}^*\right| \quad \text{(Equation 2)}$$

Other indices include Flexibility Percent Difference (or Modal Flexibility Index) and a Normalized Modal Flexibility. The latter has been shown to be statistically significant within two standard deviations and a 95% confidence interval [9].

The change detection results are plotted as three-dimensional resultants using color for quick reference. Note that the color code of green represents 0-30% relative change in a gradation to black representing 90-100% relative change. These thresholds are arbitrarily selected using personal inspection experience considering false positives and negatives. Here, an all green result translates to a noisy result where no appreciable change was detected. An all-black result would cause undue alarm, but a 100% relative decrease in flexibility does not mean collapse is imminent. The goal is a reasonable pattern that would show inspectors where to further investigate and the situation's priority.

IV. DIAGONAL BRACING RESULTS

Almost all structures have diagonal bracing to provide lateral stability and prevent collapse. In this comparison, four cases (Configurations 1, 2, 3 and 4) are studied. Figure 3 presents sketches of the four cases; note that dashed lines act as members on hidden surfaces. Configuration 1 is the baseline unreinforced frame, which is then reinforced with two diagonal bars on its North side, generating the asymmetrical structure of Configuration 2. For Configuration 3, two additional diagonal braces were added to the South side of the frame, and lastly Configuration 4 was braced diagonally on all four sides of the building.

Frequency domain analysis reveals twenty-six matching modes up to 120 Hertz (Hz) for Configuration 1 versus 2. Between Configurations 2 and 3, twenty-eight matching modes were found, while twenty-four modes were matched between Configurations 3 and 4. Sometimes new mode shapes appear or disappear as a structure changes, so this can be a challenging process.

Mode 1 was a near zero frequency rigid body motion where the whole structure above the foundation slightly translated along the z-axis. Modes 2 (4.74 Hz) and 3 (10.75 Hz) were rigid body rotations where the structure torqued towards the x direction and z direction, respectively. Modes 4 (16.24 Hz) and 5 (19.81 Hz) were a pair of "pinching" modes where two opposite corners were pulled diagonally. In Mode 4, Southwest and Northeast corners were pinched along the z direction. In Mode 5, Southwest and Northeast corners were pinched along the x direction. The Configuration 4 did not experience this motion; future mode numbers reference those of the baseline Configuration 1. For instance, Mode 6 (22.51 Hz) occurred only in Configurations 1 through 3 as the first order bending of the y-axis columns towards to the z direction.

In general, lower modes are global motions while higher modes are local modes in which local members individually deflect. The higher frequency implies that more energy is required to make this mode shape happen. Some shape pairs also appeared in the mode sets; these mirrored modes were the same shape but in opposite directions. Theoretically, mode shapes appear in the pattern as translations, first order rotations, first order torsions, second order of rotations, second order of torsions, and so on. However, because of the structure's asymmetry and member damage, some mode shapes appear or disappear and change order.

While shapes are matched, the resulting resonant frequencies are near as well. In the lower frequency range (< 35 Hz), the highest percent frequency difference of two matching modes was 11.14% (Mode 7, Configurations 1 and 4), and the lowest frequency difference was 1.83% (Mode 8, Configurations 1 and 2). In the higher frequency range (> 35 Hz), the percent frequency difference of two matching modes ranged from 0.06% to 13.75%, corresponding to Configuration 1 Mode 37 versus Configuration 2 and Configuration 1 Mode 15 versus Configuration 4.

Comparisons were calculated with FAD included the three comparisons of Configurations 1 and 2, Configurations 2 and 3, and Configurations 3 and 4 as presented in Figure 4. This leftmost plot in Figure 4 is the FAD comparison of Configurations 1 and 2 using all matched modes. The expectation is that the North side with the two reinforcing bars should show change, and FAD on the reinforcing side does show the most difference. The change in the first floor Nodes 9, 10, and 11 were 91.05%, 94.15%, and 92.44%, respectively. Comparatively, the change in the second floor beam with Nodes 22, 23, and 24 were 85.13%, 80.33%, and 84.21%, respectively. The second floor beam was hypothesized to change most due to two new connectors, but the FAD results show less change than the first floor beam. However, the columns on this North side did show expected damage and scatter.

The middle case of Figure 4 is a comparison of Configurations 2 and 3 with added bracing on the South side. That is, Configuration 3 had reinforcement on both sides (North and South) while Configuration 2 had only bracing at the South side. The expectation is that the South side deflection should change. Change in the first floor beam's nodes 9, 10, and 11 were 55.56%, 59.11%, and 57.55%, respectively, while the second floor beam with nodes 22, 23, and 24 were 67.45%, 64.34%, and 63.77%, respectively. However, much greater damage was shown on the North side, top floor. Nodes 29 through 33 indicate a range of 90.22% to 94.45%. This is possible due to dominant structural asymmetry, but it would certainly confuse an inspector as to the true change.

The rightmost plot of Figure 4 presents the FAD comparison of Configurations 3 and 4. The main differences of the two cases were the West and East side bracings. Results showed that the top floor is more changed than the second and first floors, which means that bracing all sides caused the top floor to be the least stiff entity. The change in the top floor's corner nodes 41, 37, 29, and 33 varied from 90.13% to 94.22%. Change on the second floor was less even though it experienced the same number of reinforcing connections. The second floor corner nodes 25, 21, 16, and 13 changed 54.32% and 57.11%.

The resultant of FAD is calculated as the root mean square of x, y, and z components. Nodes 1, 2, 3, and 4 were the four corners of the foundation at the bottom of each column, and Nodes 29, 33, 37, and 42 were the four top floor corners. Note that the axial modes of the y direction (vertical direction) are much stiffer than the planar X-Z motions, which FAD captures with a variation of up to 10^33. Comparing the foundation with the top floor, the y direction did not vary significantly, but the planar coordinates showed an expected large variation. In the x direction, the top floor versus foundation showed from 10^10 to 10^20 times difference, and the y direction showed from 10^17 to 10^22 times difference.

V. TWO-FACED BRACING RESULTS

In this comparison, three cases (Configurations 1, 3 and 9) are studied. Only the North and South sides of the baseline structure were reinforced in this order to test detection efficiency on symmetric systems. Both single diagonal and diagonal "cross" bracing were employed for two-faced cases, the southern and northern sides (Configurations 3 and 9 in Figure 5; dashed lines are hidden members on hidden surfaces). Conceptually, Configuration 9 would be able to carry more lateral static load than Configuration 3 while Configuration 1 would be weakest for carrying lateral load. However, along with mass and stiffness, damping is a major dynamic factor in structural deflections. Damping greatly varies based upon bar connections: in the experimental structure, for instance, a bolt at the intersection was used to connect the two bars to create the cross bracing for Configuration 9. Cross bracing, or more commonly called X-bracing, occurs when an open bay is reinforced by two diagonal braces. Notre that for these runs, internal member connections are assumed perfectly fixed.

Twenty-two matching modes exist between Configurations 1 and 3, 23 matching modes between Configurations 3 and 9, and 16 matching modes between Configurations 1 and 9. The first six modes are global modes where the whole structure deflects while higher frequency modes are generally local modes in which only beams move. Most matching modes increase in frequency with increasing reinforcement, but exceptions include the low frequency Modes 2, 3, and 6. Note that matching modes was more difficult because the bracing(s) mode more significant structural changes, causing some modes to appear and disappear.

FAD results using all matching modes are plotted in Figure 6. The leftmost plot of this figure compares Configuration 1 versus 3, and the results show as expected that the North and South side beams experienced more reinforcement. The columns have good color scatter, and the most change occurs at the top floor. The FAD detection results on the South side at the second floor (Nodes 22, 23, and 24) were 58.18%, 46.76%, and 48.34%, while the third floor Nodes 38, 39, and 40 were 92.32%, 91.37%, and 92.34%, respectively. The FAD detection results on the North side at the second floor (Nodes 14, 15, and 16) were 55.26%, 47.23%, and 46.74%, while the third floor Nodes 30, 31, and 32 were 92.46%, 93.23%, and 92.67%, respectively.

Configurations 3 and 9 are contrasted in the middle plot of Figure 6. The FAD minimum change location is unexpectedly the top floor, and the FAD maximum change location was the foundation, which should show minimal difference.

The rightmost plot of Figure 6 shows the cumulative comparison of Configuration 1 versus Configuration 9. This result is unexpected but plausible if full cross bracing most reinforces the foundation. All four-foundation points were red (70%-90% change) in this case.

In short, FAD change detection is suspect in these cases. It is likely that FAD could not properly detect changes due to its high sensitivity. The bracing(s) cause major changes in the frame along with its mode shapes and natural frequencies.

VI. CROSS BRACING RESULTS

In this comparison, three cases (Configurations 1, 8 and 9) are studied. The baseline of Configuration 1 is herein augmented with North side X-bracing for Configuration 8 and additionally with South side X-bracing for Configuration 9 (Figure 7; dashed lines are hidden members on hidden surfaces). This comparison is similar to the diagonal bracing comparison but with the stronger reinforcement of X-bracing. Thus, this run is a sensitivity study that also contrasts structural symmetry.Note that Configurations 5, 6, and 7 are not employed in any of this work.

Forty mode shapes up to 110 Hz were used to match modes. The first seven modes are global modes under 35 Hz. Twenty-three matching modes exist between Configurations 1 and Configuration 8, 24 modes between Configurations 8 and 9, and 21 modes between Configurations 1 and 9.

Figure 8 presents the FAD results for cross bracing using all modes. The leftmost plot is the sequential comparison of Configuration 1 versus 8, where the structural difference is the cross bracing on the South side. The change detection is dominant on the South side as expected. However, the South side's top floor beam shows blue (30% to 50% change), which seems low. The FAD detection result on the South side at the first floor (Node 10) was 94.38%. South side FAD values at the second floor (Nodes 22, 23, and 24) were 86.54%, 91.77%, and 88.37%, while the third floor Nodes 38, 39, and 40 were 47.74%, 47.23%, and 48.46%, respectively.

The middle plot in Figure 8 compares Configuration 8 versus 9, where the North side is sequentially cross-brace. The South side appears most reinforced and thus most changed, but this is not the location of the new bracing. The South side FAD values at the second floor (Nodes 14, 15, and 16) were 45.36%, 46.53%, and 45.76%, while the third floor Nodes 30, 31, and 32 were 84.43%, 85.32%, and 84.74%, respectively.

The rightmost plot in Figure 8 is the cumulative comparison of Configuration 1 versus 9, where the structural differences are the cross bracing on both North and South sides. The foundation appears most changed (maximum 94.56%) with reasonable color scatter decreasing towards the top. The FAD detection results at the second floor on the South side (Nodes 22, 23, and 24) were 62.14%, 63.73%, and 64.34% while on the North side (Nodes 14, 15, and 16) were 55.28%, 56.26%, and 56.77%, respectively. The FAD results at the third floor on the South side (Nodes 38, 39, and 40) were 13.32%, 12.34%, and 11.34% while on the North side (Nodes 30, 31, and 32) were 13.29%, 12.26%, and 13.62%, respectively.

VII. CONCLUSION

The motivations of this study include high profile collapses, imprecise structural inspections, poor infrastructure conditions, and limited repair resources. The goal is to augment inspection techniques to reduce their cost, time, and subjectivity. Frequency domain information was extracted from ABAQUS models and combined with the Flexibility Absolute Difference (FAD) index.

Using a total of 1,872 runs, FAD showed that diagonal bracing can induce a relative change of up to 94%, with an estimate of 60% on average. The cross-bracing performed the next highest with an estimate of 50% on average. The two-faced bracing appeared to have the lowest FAD response, with relative variations between 10% and 30%.

Short return period inspections were investigated as sequential damage cases, and longer-term inspections of cumulative damages cases generally show a detection decrease of 10% on average. Overall, this study shows promising FAD results for steel frames and provides a methodology to evaluate indicator performance. Certainly, full scale structural data analysis is necessary, especially since FAD shows generally better results when low frequency modes are included.

REFERENCES

[1]. Ahsan Zulfiqua, "Design of Bridge Inspection System (BIS) to Reduce Time and Cost," Thesis, George Mason University, October 8, 2014.

[2]. U.S. Department of Transportation Federal Highway Administration, "Bridges & Structures, Unit Cost," 02/02/2016, https://www.fhwa.dot.gov/bridge/nbi/unit_cost.cfm, Accessed April 24, 2017.

[3]. Ethan R. B. Baker and Elizabeth K. Ervin, "Identification of Global Shoring Effects on a Laboratory Steel Frame," Sustainable and Resilient Infrastructure, 2(2017) 86-96.

[4]. Spatial Technology, Inc. ACIS, ABAQUS User's Manual, Hibbitt, Karlsson & Sorensen, Inc, Pawtucket Rhode Island, 2000.

[5]. Mathworks, Inc. MATLAB: The Language of Technical Computing, Natick, Massachusetts, 1997.

[6]. Sim Han Sung, Ki Young Koo, and Hyung Jo Jung, "Modal Flexibility Based Damage Detection of Cantilever Beam Type Structure using Baseline Modification," Sound and Vibration, (2014) 4123-4138.

[7]. Ki Young Koo, J. J. Lee, and C. B. Yun, "Damage Detection of Bridge Structure using Modal Flexibility under Temperature Variations," The International Federation of Automatic Control, Seoul, Korea, July 6-11, 2008.

[8]. Samantha M. Sabatino, "Experimental Damage Diagnosis of a Model Three-Story Spatial Frame," Thesis, University of Mississippi, Oxford, Mississippi, May 2011.

[9]. Zong Sun, Jan Ming Ko, and Yi Qing Ni, "Modal Indices for Identifying Damage Location in Cable-Stayed Kap Shui Mun Bridge," Health Monitoring and Management of Civil Infrastructure Systems, (2011)379- 389. `IEA: World Energy Outlook 2009. International Energy Agency Publications (2008).

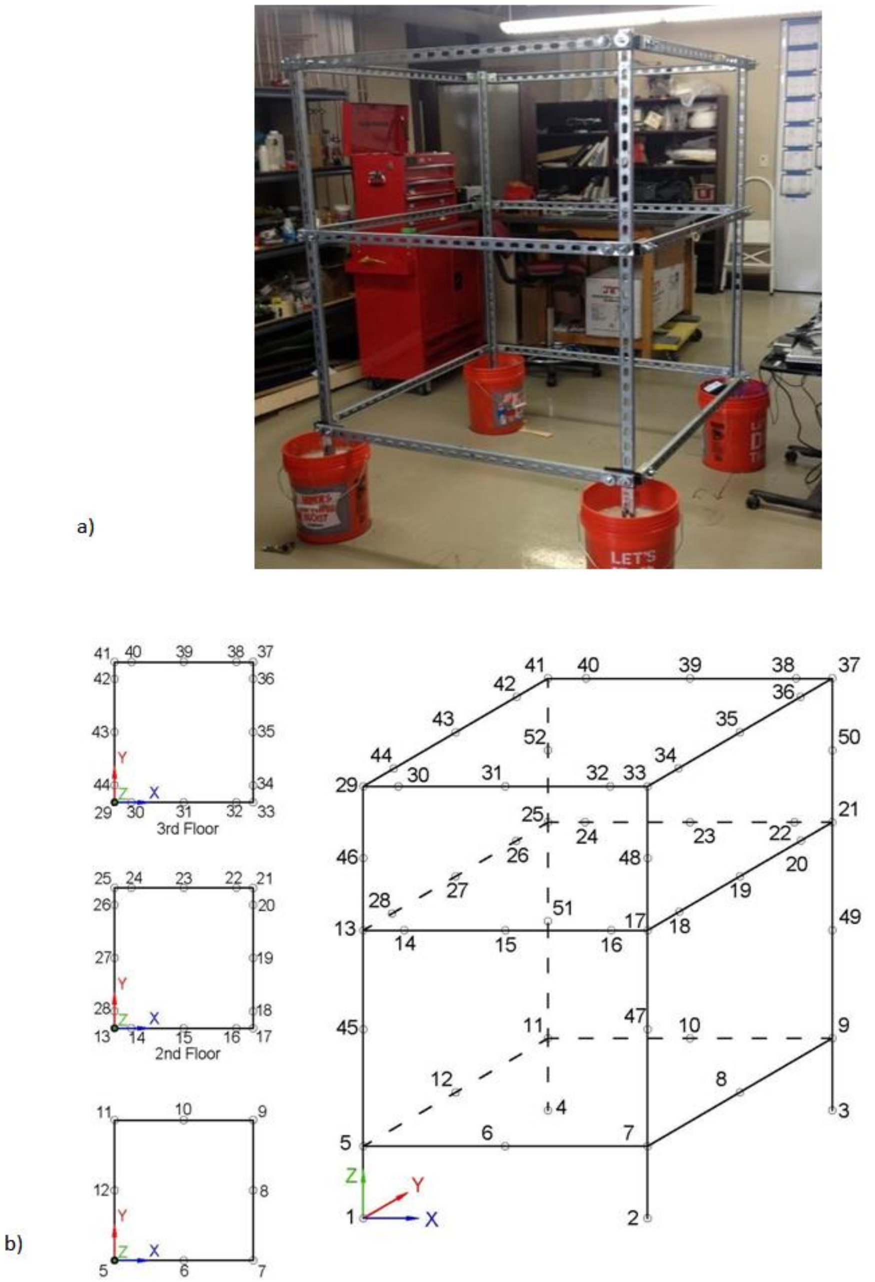

Fig. 1. Experimental Frame a) Geometry b: Node Numbering

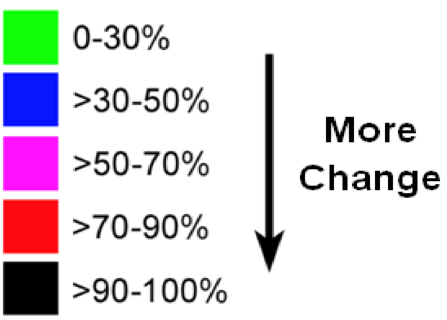

Fig. 2. Color Code for Easy Identification of Change;*note thresholds are arbitrary*.

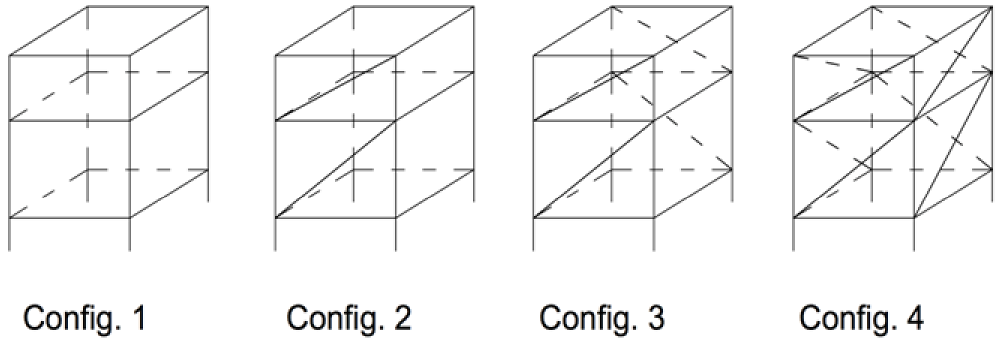

Fig. 3. Diagonal Bracing Cases

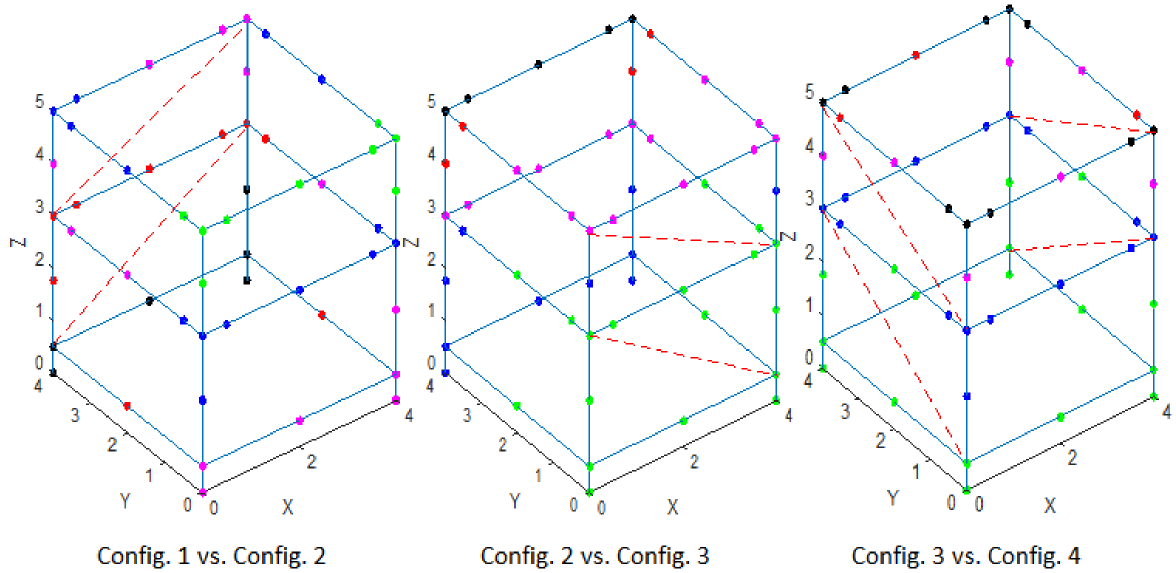

Fig. 4. FAD Detection Results for Sequential Diagonal Bracing
Dotted lines represent bar changes.

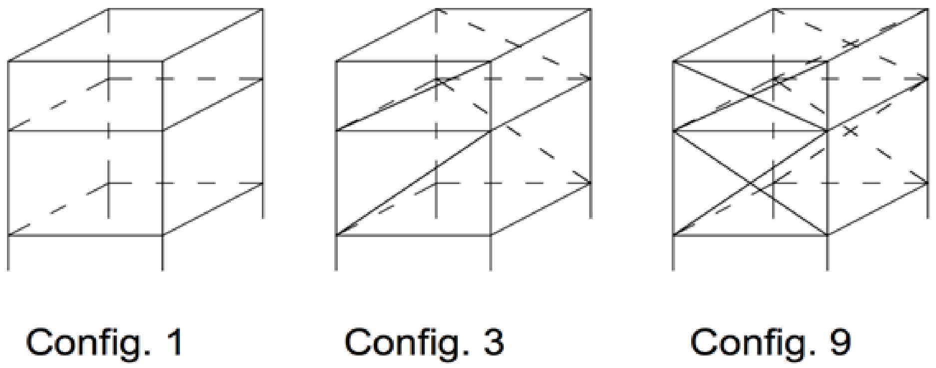

Fig. 5. Two-Faced Bracing Cases

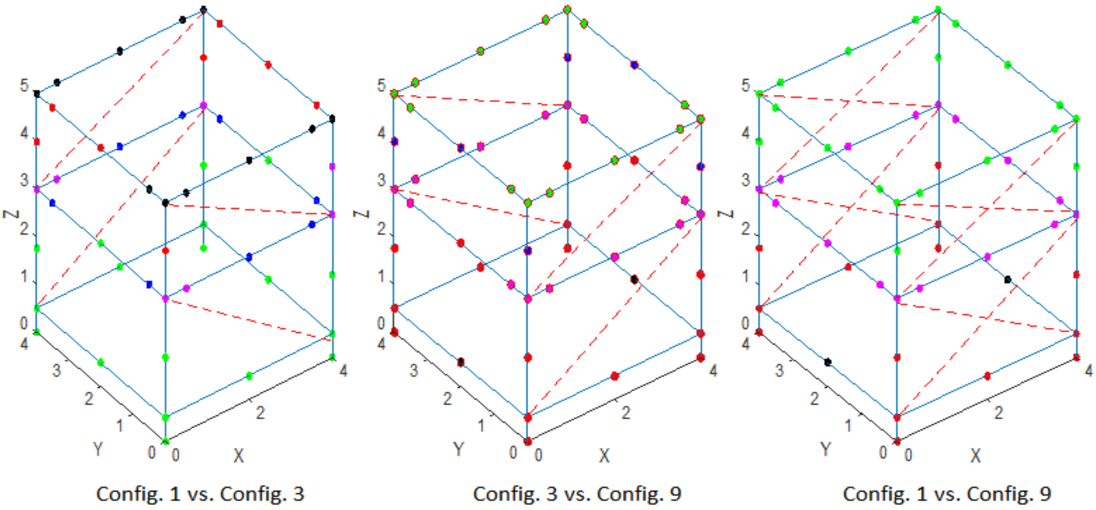

Fig. 6. FAD Detection Results for Two-Faced Bracing
Dotted lines represent bar changes.

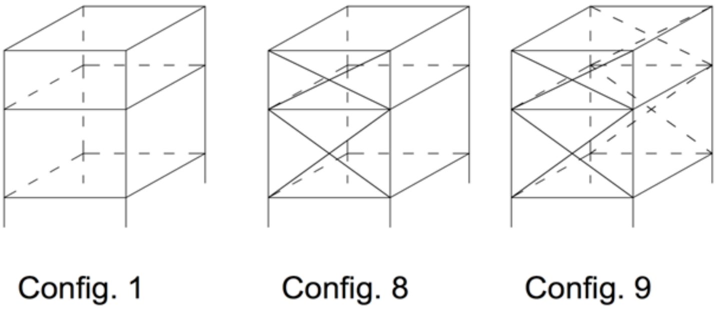

Fig. 7. Cross or X-Bracing Cases

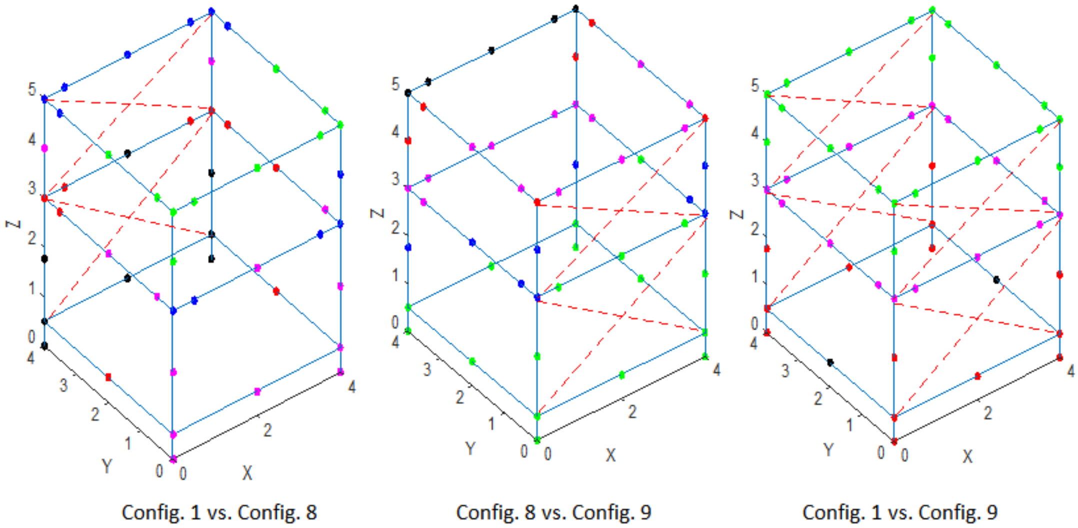

Fig.8. FAD Detection Results for Cross-Bracing
Dotted lines represent bar changes.

Ai D. Nguyen and Elizabeth K. Ervin, "Use of Flexibility Absolute Difference Index to Detect Bracing Effects in a Steel Frame Model,"American Journal of Engineering Research (AJER), vol.8, no.03, 2019, pp.107-114.